



Quark mass dependence of the pion vector form factor

Feng-Kun Guo^a, Christoph Hanhart^{a,b,*}, Felipe J. Llanes-Estrada^c, Ulf-G. Meißner^{a,b,d}

^a Institut für Kernphysik and Jülich Center for Hadron Physics, Forschungszentrum Jülich, D-52425 Jülich, Germany

^b Institute for Advanced Simulation, Forschungszentrum Jülich, D-52425 Jülich, Germany

^c Departamento de Física Teórica I, Universidad Complutense de Madrid, 28040 Madrid, Spain

^d Helmholtz-Institut für Strahlen- und Kernphysik (Theorie) and Bethe Center for Theoretical Physics, Universität Bonn, D-53115 Bonn, Germany

ARTICLE INFO

Article history:

Received 8 January 2009

Received in revised form 23 April 2009

Accepted 7 May 2009

Available online 28 May 2009

Editor: J.-P. Blaizot

PACS:

11.10.St

11.55.Bq

12.39.Fe

12.40.Vv

13.40.Gp

Keywords:

Pion form factor

Omnès representation

Quark mass dependence

Inverse amplitude method

ABSTRACT

We examine the quark mass dependence of the pion vector form factor, particularly the curvature (mean quartic radius). We focus our study on the consequences of assuming that the coupling constant of the ρ to pions, $g_{\rho\pi\pi}$, is largely independent of the quark mass while the quark mass dependence of the ρ mass is given by recent lattice data. By employing the Omnès representation we can provide a very clean estimate for a certain combination of the curvature and the square radius, whose quark mass dependence could be determined from lattice computations. This study provides an independent access to the quark mass dependence of the $\rho\pi\pi$ coupling and in this way a non-trivial check of the systematics of chiral extrapolations. We also provide an improved value for the curvature for physical values for the quark masses, namely $\langle r^4 \rangle = 0.73 \pm 0.09 \text{ fm}^4$ or equivalently $c_V = 4.00 \pm 0.50 \text{ GeV}^{-4}$.

© 2009 Elsevier B.V. All rights reserved.

1. Introduction and notation

The expectation value of the vector current between two pion fields may be written as

$$\langle \pi^\pm(p') | j^\mu | \pi^\pm(p) \rangle = (p + p')^\mu F_\pi^V(q^2).$$

Since the only form factor that we discuss is the charged pion form factor, we will denote it simply as $F(q^2)$, where $q = p - p'$. It is conventionally normalized as $F(0) = 1$.

An expansion around zero momentum transfer allows for a physical interpretation of the form factor in terms of the pion's rest frame charge density $\rho(r)$, given by

$$F(t) = 1 + \frac{1}{3!} \langle r^2 \rangle_\rho t + \frac{1}{5!} \langle r^4 \rangle_\rho t^2 + \mathcal{O}(t^3). \quad (1)$$

Here we used the notation of Ref. [1]. Alternatively, the curvature c_V^π of the form factor may be introduced as the coefficient of the t^2 -term [2] which leads to

$$c_V^\pi = \frac{1}{5!} \langle r^4 \rangle. \quad (2)$$

The first term in the form factor expansion is the conventional charge normalization $\int d^3r \rho(r) = \langle 1 \rangle_\rho = 1$, and the derivative at the origin provides the (vector or charge) pion radius $\langle r^2 \rangle = 6(dF/dq^2)(0)$. At the next order, the non-relativistic interpretation should be modified as effects of boosting the pion wave function should begin to appear. In this article we will ignore this subtlety, and simply use equivalently the term pion's mean quartic radius or form factor curvature. We will mainly focus on this quantity. Using both chiral perturbation theory and dispersion relations we find a reliable value for the curvature.

Assuming that the $\rho\pi\pi$ coupling is largely independent of the quark masses for a given quark mass dependence of m_ρ , we can also predict the quark mass dependence of the curvature. The quark mass dependence of the ρ properties was studied in various recent lattice simulations [3,4] as well as using chiral perturbation

* Corresponding author at: Institut für Kernphysik and Jülich Center for Hadron Physics, Forschungszentrum Jülich, D-52425 Jülich, Germany.

E-mail address: c.hanhart@fz-juelich.de (C. Hanhart).

Table 1

Theory estimates of the pion's quartic radius.

$\langle r^4 \rangle / \langle r^2 \rangle^2$	Method
3.3	VMD [2]
2 ± 2.5	Lattice $m_\pi = 0.33$ GeV [16]
3.0 ± 0.5	Lattice [17]
3.5 ± 0.5	NNLO χ PT [18]
3.1 ± 0.4	Padé approximants [19]
3.6 ± 0.6	Eq. (5), this work

theory with explicit spin-1 fields [5] and also unitarized chiral perturbation theory [6].

Abundant data on the pion form factor can be obtained from the Durham reaction database. For the timelike form factor we use contemporary sets from the CMD2, KLOE, and SND experiments [7–9]. In addition there is higher energy data from BaBar [10] that shows the $\rho(1700)$ and a shoulder that could correspond to the $\rho(1400)$. However, we employ only the $\rho(770)$ and will therefore not extend our study beyond 1.2 GeV, where in addition $\pi\omega$ and other inelastic channels start to contribute significantly. It is this condition that prevents us from studying the radius instead of the curvature, as will be explained below.

In the case of the spacelike pion form factor the data is taken from the CERN NA7 Collaboration [11]. The more recent data from JLAB [12] was taken at values of Q^2 too large for our study. For a recent review on the status of the spacelike form factor see Ref. [13].

The two-loop chiral perturbation theory (χ PT) analysis of [14] yielded a mean quadratic radius of

$$\langle r^2 \rangle = 0.452(13) \text{ fm}^2, \quad (3)$$

which is the currently accepted value [15]. In order to get a feeling on what to expect for the quartic radius, we start with some simple classical examples. For this discussion we will divide it by the mean square radius squared, the resulting ratio $R \equiv \langle r^4 \rangle / \langle r^2 \rangle^2$ quantifies the radial spread of the charge distribution. For a charge conducting sphere the spread is minimal with $R = 1$ (all the charge is at the surface), and for a uniformly charged dielectric sphere $R = 25/21$. On the other hand, the ratio is as large as $5/2$ for a charge distribution with an exponential dependence on the radius e^{-mr} . A vector-meson pole form factor $F(t) = (1 - t/m_\rho^2)^{-1}$ gives an even higher value of $10/3$ [2].

Some results about the pion's quartic radius, including this work, are collected in Table 1. Furthermore, after having analyzed the pion em form factor data by using analyticity, the curvature was constrained in the range $[0.25 \text{ GeV}^{-4}, 7.57 \text{ GeV}^{-4}]$ in Ref. [20] and $[2.3 \text{ GeV}^{-4}, 5.4 \text{ GeV}^{-4}]$ in a very recent analysis [21]. Of particular interest for us, and for a lattice determination, is the quark mass dependence, or m_π dependence, of the quartic radius – quark and pion mass dependences are interchangeable thanks to the Gell-Mann–Oakes–Renner relation $m_\pi^2 f_\pi^2 = -2\hat{m}_q \langle \bar{q}q \rangle$, where f_π denotes the pion decay constant, $\hat{m} = (m_u + m_d)/2$, and $\langle \bar{q}q \rangle$ is the chiral condensate. A study of this within chiral perturbation theory would require control of the N³LO Lagrangian, the quartic radius being NNLO itself, and this seems out of today's reach.

We examine the problem with the simplifying assumption that $g_{\rho\pi\pi}$ is m_π -independent while the m_π dependence of m_ρ is taken from other sources. To control the model dependence, we employ the Omnès representation of the form factor, sketched in Section 2.1 below. In the absence of form factor zeroes, and neglecting inelastic channels, this only requires knowledge of the elastic pion–pion scattering phase shifts. We parameterize them, with a simple Breit–Wigner model described in Section 2.2. Since this model contains $g_{\rho\pi\pi}$ and m_ρ as the only parameters, the above assumption can be employed in a straightforward way. In addition we also use

the predictions of unitarized chiral perturbation theory for both rho mass and coupling. The resulting quark mass dependence of the rho properties was investigated in Ref. [6]. Using this alternative parameterization we get almost identical results. The pion mass dependence of the curvature turns out to be similar to that of the square radius.

The chiral Lagrangian, known to a limited order, is not employed to make an expansion in powers of momentum of the form factor. The task of fixing the curvature at the physical point is left to the experimental phase-shift data and analyticity (through the Omnès relation). The chiral Lagrangian can then be conveniently employed for the quark mass dependence. Rigorously, the extracted mass dependence is LO over the entire momentum region considered, since these are the terms of the Lagrangian that are independent of momenta. However, the IAM being constructed at NLO, one hopes to include the most important higher order terms in the quark mass dependence.

2. Omnès representation of the form factor

2.1. Phase-shift representation of the quartic radius

The Omnès equation [22] encodes the analyticity properties of the pion form factor $F(s)$, that has an elastic unitarity cut on the positive s -axis for $s \in (4m_\pi^2, \infty)$, and is otherwise analytic. Further superimposed cuts due to inelastic channels are neglected in its derivation, and the form factor is assumed to have no zeroes (which, as we know today, is phenomenologically correct). We have explored the possibility of zeroes in the complex plane by analytically continuing the experimental data with the help of the Cauchy–Riemann equations [23]. For a small band around the real axis, they can be excluded. Some remarks on inelastic channels can be found in [24].

From $\text{Im}(F) = \tan \delta_{11} \text{Re}(F)$, which relates the discontinuity in the vector form factor to the elastic scattering phase shift in the vector–isovector channel, one can obtain an unsubtracted Omnès relation thanks to the QCD counting rules [25]. This holds only as a matter of principle, since the QCD counting rules apply only when elastic scattering is irrelevant by the numerous inelastic channels open. We only wish to use low energy input (up to 1.2 GeV) and we will therefore use a subtracted dispersion relation and cut the high energy contributions with a cutoff. The variation of the results with this cutoff provides a systematic uncertainty in our work, which, as a consequence of the subtraction, turns out to be moderate. Due to this we cannot provide a strong prediction for $\langle r^2 \rangle(m_\pi)$. Instead we subtract the equation once more reducing the cutoff dependence, building-in the correct $\langle r^2 \rangle(m_\pi)$ and its χ PT m_π dependence by construction, and make instead a prediction for the curvature.

If there are no bound state poles, as is the case of $\pi\pi$ scattering for physical quark masses, nor the form factor vanishes anywhere in the complex plane, as we presume for $F(t)$, the celebrated Omnès relation provides a representation of the form factor in terms of the scattering phase (we give some more detail in [26]). We will use a twice subtracted version

$$F(t) = \exp \left(P_1 t + \frac{t^2}{\pi} \int_{4m_\pi^2}^{\infty} ds \frac{\delta_{11}(s)}{s^2(s-t-i\epsilon)} \right). \quad (4)$$

Note, the normalization condition of the form factor prohibits a constant term in the exponent. The constant P_1 can be identified with the square radius of the pion $P_1 = \langle r^2 \rangle / 6$. This representation of the form factor has been used in the literature, see for example [27].

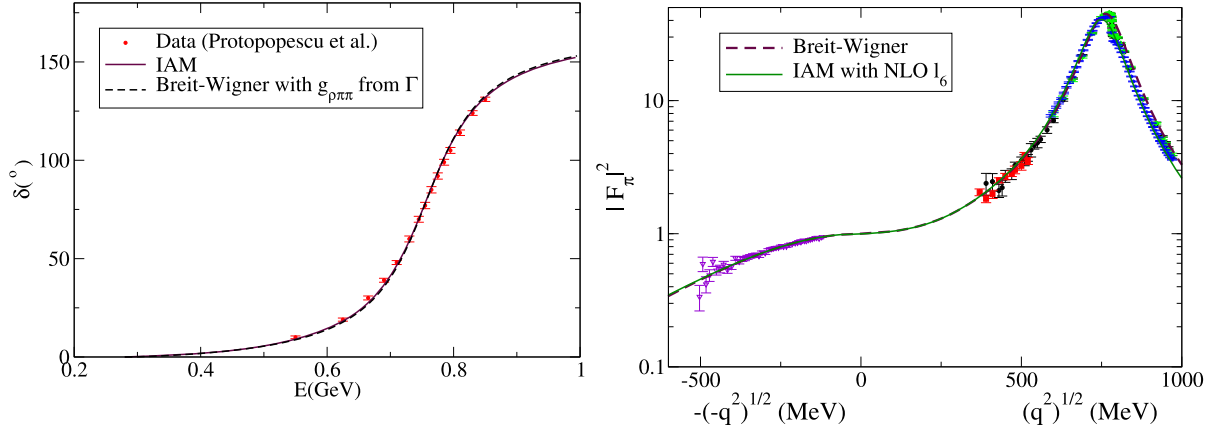


Fig. 1. The scattering phase in the vector channel (left) for the Breit-Wigner model (dashed line) and the Inverse Amplitude Method (solid line). We also plot the square form factor modulus (right). To be able to plot the spacelike and timelike data together, the first is plotted against the unphysical variable $-\sqrt{-q^2}$ with q^2 the (negative) spacelike momentum transfer. Here we use $\langle r^2 \rangle$ as input as described in the text.

Recalling the definition of the curvature of the pion form factor (cf. Eq. (2)) we may read off an expression for c_V^π directly from Eq. (4):

$$c_V^\pi = \frac{\langle r^4 \rangle}{120} = \frac{1}{72} \langle r^2 \rangle^2 + \frac{1}{\pi} \int_{4m_\pi^2}^{\infty} ds \frac{\delta_{11}(s)}{s^3} \quad (5)$$

which is quite a beautiful formula, since it allows a third independent extraction of the curvature c_V^π besides NNLO χ PT or a fit to spacelike data beyond the linear fall in t where uncertainties get large. Instead we employ only the elastic phase shift. In addition, since the quantity

$$\tilde{c}_V^\pi \equiv c_V^\pi - \frac{1}{72} \langle r^2 \rangle^2 \quad (6)$$

is described solely in terms of the $\pi\pi$ p -wave phase shifts, its quark mass dependence is closely linked to that of the ρ -meson properties. This relation is analogous to others existing for the mean-square radius [2,28].

2.2. A simple Breit-Wigner model

To estimate the form factor based on the Omnès representation, we employ a simple relativistic Breit-Wigner model of the scattering amplitude, in which an s -channel resonance dominates the scattering

$$a_{11}(s) = \frac{c}{s - m_\rho^2 - im_\rho \Gamma_{\text{tot}}(s)}, \quad (7)$$

where Γ_{tot} is the total width of the ρ resonance, that reads

$$\Gamma_{\text{tot}} = \frac{g_{\rho\pi\pi}^2 p^3}{6\pi m_\rho^2} = \frac{g_{\rho\pi\pi}^2 (\frac{s}{4} - m_\pi^2)^{3/2}}{6\pi m_\rho^2}. \quad (8)$$

Here c is an irrelevant constant that may be expressed in terms of m_ρ and Γ_{tot} . We may write

$$\delta_{11}(s) = \arctan \frac{\text{Im} a_{11}(s)}{\text{Re} a_{11}(s)} = \arctan \frac{m_\rho \Gamma_{\text{tot}}(s)}{m_\rho^2 - s}. \quad (9)$$

With this phase variation the integral representation converges without additional subtractions (although the high-energy tail is ad-hoc), however, even values as large as $s = 7 \text{ GeV}^2$ contribute to the integral.

A good fit can be seen in Fig. 1 for the phase shift and square form factor modulus. To produce the figures we use $m_\pi^{\text{phys}} = 139 \text{ MeV}$, $m_\rho = 775 \text{ MeV}$, $\Gamma_\rho^{\text{phys}} = 150 \text{ MeV}$ (to determine $g_{\rho\pi\pi}$). Other unitarization approaches give results of similar quality, see, e.g., Ref. [29].

Using the formula given above we may now extract the curvature directly from the elastic pion phase shifts, using the square radius as input. We find

$$c_V^\pi = 3.75 \pm 0.33 \text{ GeV}^{-4}, \quad \langle r^4 \rangle = 0.68 \pm 0.06 \text{ fm}^4, \quad (10)$$

where the uncertainty contains both the uncertainty in $\langle r^2 \rangle$ and the systematic uncertainty introduced by evaluating the integral only up to finite values (we allow a large range from 1 GeV to 16 GeV for the variation of the cutoff, although the integral is basically converged for a cutoff of 2 GeV). The curvature agrees to that from vector meson dominance which is about 3.5 GeV^{-4} [2] and it is consistent with the constraint $[2.3 \text{ GeV}^{-4}, 5.4 \text{ GeV}^{-4}]$ from analyzing the form factor data using analyticity [21]. The advantage of our analysis is that it allows in addition for a controlled estimate of the uncertainty.

As mentioned above we will investigate the quark mass dependence of the pion form factor based on the assumption that $g_{\rho\pi\pi}$ is independent of the quark mass with the quark mass dependence of m_ρ taken from other sources. Since both parameters are explicit in the parameterization given above, we may study the resulting quark mass dependence of c_V^π , once that of $\langle r^2 \rangle$ is fixed.

3. Chiral perturbation theory

We start by giving the chiral expansion of the vector form factor [30] valid to NLO in χ PT,

$$F(t) = 1 + \frac{1}{6f_\pi^2} (t - 4m_\pi^2) \bar{J}(t) + \frac{t}{96\pi^2 f_\pi^2} \left(\bar{l}_6 - \frac{1}{3} \right), \quad (11)$$

$$\bar{J}(t) = \frac{1}{16\pi^2} \left[\sigma \log \left(\frac{\sigma - 1}{\sigma + 1} \right) + 2 \right],$$

with $\sigma = \sqrt{1 - 4m_\pi^2/t}$ (we are free to change M, F to the physical m_π, f_π , since the difference is of NNLO). A common strategy is to fix the \bar{l}_6 constant from the square charge radius [30]

$$\langle r^2 \rangle = \frac{1}{16\pi^2 f_\pi^2} (\bar{l}_6 - 1), \quad (12)$$

which is correct up to $\mathcal{O}(m_\pi^2)$ in χ PT. Higher orders in the chiral expansion cannot bring in powers of t since, by definition, the

charge squared radius is proportional to the coefficient of the term linear in t in the form factor. However, they can bring additional constants to the right-hand side (each of a natural order suppressed by additional factors of $1/(4\pi f_\pi)^2$), and, more important for our purposes, a polynomial of m_π^2 . To make sure we are not eschewing a critical m_π dependence, we will compare the right-hand side of Eq. (12) with the NNLO correction in chiral perturbation theory [18]. The NLO result Eq. (12), that depends only logarithmically on the pion mass (see Eq. (16) below), is then extended to

$$\langle r^2 \rangle = \frac{1}{16\pi^2 f_\pi^2} \left[\left(1 + \frac{m_\pi^2}{8\pi^2 f_\pi^2} \bar{l}_4 \right) (\bar{l}_6 - 1) + \frac{m_\pi^2}{16\pi^2 f_\pi^2} \left(16\pi^2 \frac{13}{192} - \frac{181}{48} \right) \right] \quad (13)$$

with

$$\bar{l}_6 = \bar{l}_6 + 6 \frac{m_\pi^2}{f_\pi^2} \left[16\pi^2 r_{V1}^r(\mu^2) + \frac{1}{48\pi^2} \log\left(\frac{m_\pi^2}{\mu^2}\right) \left(\frac{19}{12} - \bar{l}_1 + \bar{l}_2 \right) \right], \quad (14)$$

where r_{V1}^r is a counterterm to be determined empirically, and we will use the simple VMD estimate from the same work, at the ρ scale,

$$r_{V1}^r(m_\rho^2) \simeq -0.25 \times 10^{-3}.$$

With this estimate, those authors find

$$\bar{l}_6 = \bar{l}_6 - 1.44$$

(the scale-dependence of this number cancels in Eq. (14)). The estimate is taken with constants corresponding to set I that we copy in Table 2).

Here we have to recall the pion mass dependence of the \bar{l} 's. The l_i , as coefficients of the expansion in powers of m_π^2 of the Lagrangian density, are by definition pion-mass-independent, and so are their renormalized counterparts \bar{l}_i^r . However, the barred quantities are related to them by absorbing a chiral logarithm

$$\bar{l}_i^r = \frac{\gamma_i}{32\pi^2} \left[\bar{l}_i + \log\left(\frac{m_\pi^2}{\mu^2}\right) \right] \quad (15)$$

that makes the \bar{l} 's scale-independent, but in exchange, pion-mass-dependent. This dependence needs to be kept track of in the calculation. It becomes crucial in the chiral limit when the pion radius diverges due to the virtual pion cloud becoming long-ranged as the pion mass vanishes. This effect appears through \bar{l}_6 .

Therefore, we denote by \bar{l}_i^{phys} the value that the low energy constants take by fitting to physical-world data. From here on, when varying the quark (or pion) mass, one needs to change the constant according to

$$\bar{l}_i = \bar{l}_i^{\text{phys}} - \log\left(\frac{m_\pi^2}{(m_\pi^{\text{phys}})^2}\right). \quad (16)$$

The quark mass dependence of the square radius, needed as a subtraction, is also taken from χ PT. Clearly, the curvature c_V^π as well as its quark mass dependence, could also be determined in χ PT directly. Depending on the fit and systematics chosen in Ref. [18], which is two-flavor $\mathcal{O}(p^6)$ χ PT calculation, its value could vary between $2\text{--}6 \text{ GeV}^{-4}$, although the authors quote a value around 2.25 GeV^{-4} , in agreement with a previous estimate [2]. By fitting to form factor data, they obtain 3.85 GeV^{-4} , and this result we copy into Table 1. A $\mathcal{O}(p^6)$ fit in three-flavor χ PT leads to a range $4.49 \pm 0.28 \text{ GeV}^{-4}$ [14].

Table 2

Values of the low-energy constants of the NLO $SU(2)$ chiral Lagrangian. We employ the last row in the calculation. For comparison we give several well-known sets. The error refers to the last significant figure. These are determinations based on data alone. Several phenomenological and theoretical predictions based on semi-analytical approaches (large N_c , Dyson–Schwinger, resonance saturation, etc.) can be found in the literature [34].

LEC	\bar{l}_1	\bar{l}_2	\bar{l}_3	\bar{l}_4	\bar{l}_6
Gasser–Leutwyler [30]	-2 ± 4	6 ± 1.3	2.9 ± 2.4	4.3 ± 0.9	16 ± 1
CGL [36]	-0.4 ± 0.6	4.3 ± 0.1		4.4 ± 0.2	
Dobado et al. [37]	-0.6 ± 0.9	6.3 ± 0.5	2.9 ± 2.4	4.3 ± 0.9	16 ± 1
Bijnens et al. set I [18]	-1.7	6.1	2.4	4.4 ± 0.3	16 ± 1
Bijnens et al. set II [18]	-1.5	4.5	2.9	4.3	
This work	0.1 ± 1.5	6 ± 1.3	$2.9(\text{fix})$	4.3 ± 0.9	16.6 ± 0.4

With this we have all the input ready to use Eq. (5) and establish the quark mass dependence of the curvature, using the Breit–Wigner representation of the phase shifts and the given assumptions on the quark mass dependence of both the ρ mass and coupling.

However, before we proceed we introduce a second method that allows one to estimate the quark mass dependence of the ρ properties directly from the χ PT amplitudes evaluated up to a given order, namely the unitarized chiral perturbation theory or the inverse amplitude method (IAM). The representation we are going to use is consistent with NLO chiral perturbation theory at low momentum, and satisfies exact elastic unitarity, fitting the pion scattering data up to 1.2 GeV well.

One can organize the chiral expansion as

$$a_{11}(s) = a_{11}^{\text{LO}}(s) + a_{11}^{\text{NLO}}(s) + \dots, \quad (17)$$

but the series truncated at any order only satisfies elastic unitarity perturbatively. This is solved by the Inverse Amplitude Method [31] that reads (suppressing the spin and isospin subindices)

$$a^{\text{IAM}}(s) = \frac{a_{\text{LO}}^2(s)}{a^{\text{LO}}(s) - a^{\text{NLO}}(s)}. \quad (18)$$

A Taylor expansion of this amplitude returns NLO χ PT as usual for a Padé approximant. However elastic unitarity is now exact, and the possibility of a zero of the denominator allows for resonances to appear.

The associated phase shift

$$\delta_{11}^{\text{IAM}}(s) = \arctan\left(\frac{\text{Im } a_{11}^{\text{IAM}}(s)}{\text{Re } a_{11}^{\text{IAM}}(s)}\right)$$

may be directly employed for the time-like form factor through the Omnès representation. A similar procedure was taken to calculate the scalar and vector form factors of the pion [32,33].

The pion mass dependence of the ρ meson properties were studied in Ref. [6] and it was found that $g_{\rho\pi\pi}$ depends only very mildly on the quark mass. In the next section we will investigate the consequences of this finding on the pion vector form factor.

The low energy constants necessary to complete the calculation are fit to the phase shifts data and given in Table 2, where they are compared to well-known determinations. Note that with the phase shift data one can only determine the difference $\bar{l}_2 - \bar{l}_1$ which turns out to be about 6 [35]. Using Eq. (5), the curvature can then be obtained as

$$c_V^\pi = 4.00 \pm 0.50 \text{ GeV}^{-4}, \quad \langle r^4 \rangle = 0.73 \pm 0.09 \text{ fm}^4. \quad (19)$$

The quantity depending solely on the phase shift is

$$\tilde{c}_V^\pi = 2.13 \pm 0.42 \text{ GeV}^{-4}. \quad (20)$$

These values are to be considered as our results at the physical pion mass.

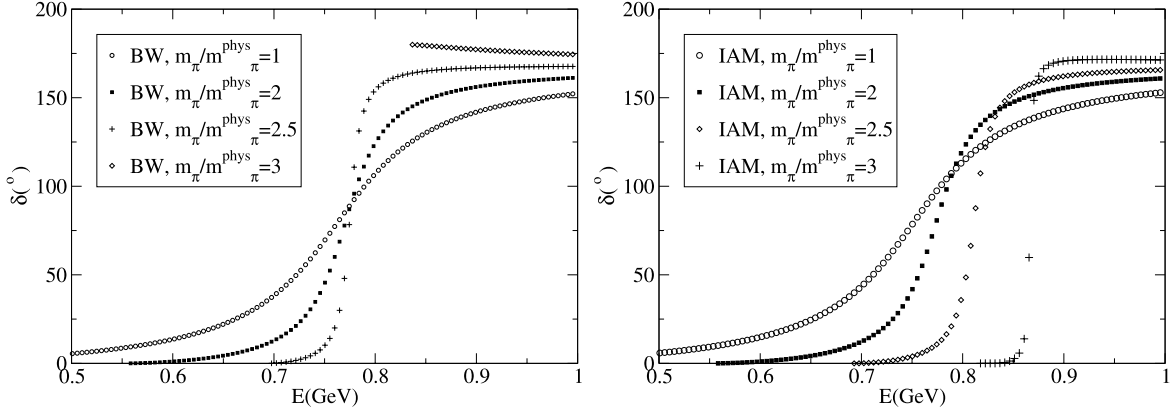


Fig. 2. Variation of the elastic $\pi\pi$ phase δ_{11} with the pion mass. Left: Breit-Wigner model. Note that for $m_\pi = 3m_\pi^{\text{phys}}$ the ρ (held at constant mass) has already crossed below the $\pi\pi$ threshold and is a bound state. Right: Inverse Amplitude Method. The resonance stays above the $\pi\pi$ threshold, its mass having a slight dependence on m_π , until rather high pion masses.

4. Study of the quark mass dependence

4.1. Mass dependence of the phase shift

In this section we study the quark mass dependence of the pion vector form factor based on both the Breit-Wigner model as well as the amplitudes from the IAM. Since quark masses are scheme-dependent and there is a one-to-one correspondence between pion masses and quark masses, $m_\pi^2 f_\pi^2 = -2\hat{m}_q \langle \bar{q}q \rangle$, it is common practice to show results as functions of the pion mass. In the left panel of Fig. 2 we plot the variation in the isospin-1 p -wave elastic $\pi\pi$ phase shift δ_{11} with the pion mass in the Breit-Wigner model, where the physical pion mass is denoted by m_π^{phys} . For small increases in the pion mass, with m_ρ being held fixed for illustration, we see how the resonance becomes narrower as the pion threshold approaches. Finally, for $2m_\pi > m_\rho$, the ρ becomes bound and the phase shift starts at 180 degrees in agreement with Levinson's theorem with one bound state.

Next we consider the IAM. Here what is held constant is the renormalized constants in the chiral Lagrangian ($l_i^r(\mu)$) since, as discussed, they are by definition independent of the pion mass. The scale-independent \bar{l} 's run logarithmically with the pion mass. This dependence and the explicit pion masses in the chiral series bring about a small m_π dependence of the ρ mass that puts it just above threshold for $m_\pi = 3m_\pi^{\text{phys}}$. We plot in the right panel of Fig. 2 the resulting phase as a function of the $\pi\pi$ invariant mass for different values of the pion mass.

The prediction of the pion mass dependence of the ρ mass resulting from the IAM is shown as the solid curve in Fig. 3. The parameters used are $\bar{l}_1 = -0.08$, $\bar{l}_2 = 5.78$, $\bar{l}_3 = 2.9$ and $\bar{l}_4 = 4.3$. In this figure we also show the results of a recent lattice study [4]. For our comparison we choose this one, for it is the simulation where the lowest pion masses are used. To allow for a comparison with recent lattice data, here the ρ mass is defined as the value of \sqrt{s} , where the $\pi\pi$ phase shift is 90° . The resulting numbers differ somewhat from those corresponding to the real part of the pole position in the second Riemann sheet – the latter definition of the mass was used in Ref. [6]. For comparison, we also show the very recent lattice data [4] as the filled circles with error bars. The agreement of the IAM with the lattice data is rather satisfying. For later use, the lattice data are fitted with an expression derived from an extended version of χPT [5]

$$m_\rho = m_\rho^0 + c_1 m_\pi^2 + c_2 m_\pi^3 + c_3 m_\pi^4 \log\left(\frac{m_\pi^2}{m_\rho^2}\right). \quad (21)$$

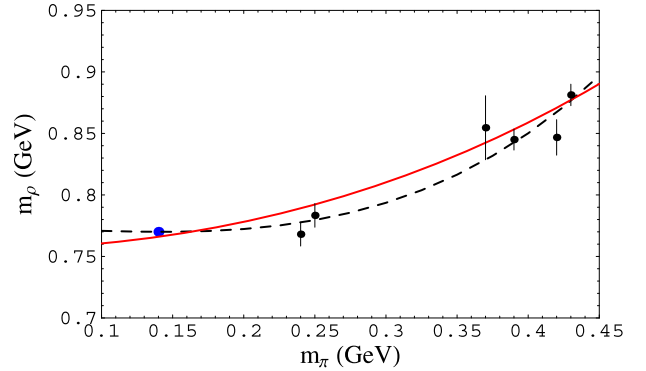


Fig. 3. Dependence of the ρ mass on the pion mass. Here the ρ mass is defined as the value of \sqrt{s} , where the $\pi\pi$ p -wave phase shifts cross 90° degrees. Shown are the result from the IAM (solid line) and a fit using Eq. (21) (dashed line) to the lattice data, shown as solid dots [4]. The lowest point is the physical ρ mass.

The parameter m_ρ^0 is not included in the fit. It is fixed by the condition that $m_\rho = 0.77$ GeV at the physical pion mass. We find for the ρ mass in the chiral limit $m_\rho^0 = 0.77 \pm 0.1$ GeV. The resulting parameters are

$$\begin{aligned} c_1 &= -0.53 \pm 0.44 \text{ GeV}^{-1}, & c_2 &= 2 \pm 1 \text{ GeV}^{-2}, \\ c_3 &= -1 \pm 3 \text{ GeV}^{-3}. \end{aligned} \quad (22)$$

Using the central values, we get the dashed curve as shown in Fig. 3. Note, the uncertainties in the parameters show some correlation, however, since we are here mainly interested in a parameterization of the lattice data, we may ignore this observation. Since the pion mass grows faster with the quark mass, eventually the ρ becomes bound (just as the J/ψ is under the $D\bar{D}$ threshold), but this happens for yet larger pion masses.

4.2. Extrapolation in NLO and NNLO chiral perturbation theory

Space-like form factors are in principle accessible on a lattice. Since these studies usually employ heavier-than-real quarks, the pion mass obtained is also higher than the physical pion mass, and an extrapolation is necessary. Another extrapolation to low momentum (due to the finite volume enclosed by the lattice) is necessary if the mean square and quartic radii are to be extracted. The mean square radius has indeed been studied before [16,38] and extrapolation to physical pion masses taken from chiral per-

turbation theory. It would be interesting to have lattice data at several quark masses to test it.

Momentum extrapolations to $q^2 = 0$ are, in view of the mean quartic radius, non-linear. In the extraction of the mean square radius, the authors of [38] quote a 10% systematic error in the lattice extraction due to $m_\pi^2/(1 \text{ GeV}^2)$ χ PT errors, and 20% due to $q_{\min}^2/(1 \text{ GeV}^2)$ momentum extrapolation errors.

The momentum extrapolation however seems to be avoidable with twisted boundary conditions for the fermion fields [16], and indeed those authors find

$$\langle r^2 \rangle_{330 \text{ MeV}} = 0.35(3) \text{ fm}^2, \quad \langle r^2 \rangle_{139 \text{ MeV}} = 0.42(3) \text{ fm}^2,$$

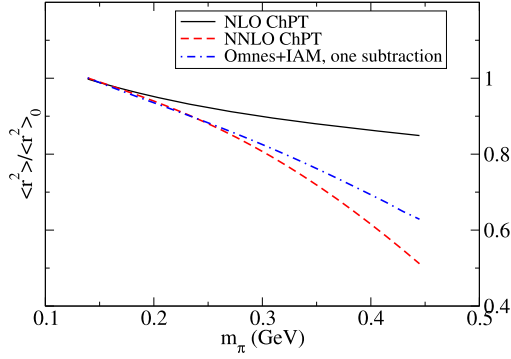


Fig. 4. Pion mass dependence of the mean square radius, based on NLO and NNLO Chiral Perturbation Theory, with r_{V1}' fixed at its VMD value (its pion mass dependence contributing at NNNLO is neglected). Also plotted is the mass dependence resulting from a once-subtracted Omnès representation. The data is normalized to the radius for physical pion mass.

where the value at the physical pion mass is obtained with the help of the NLO $SU(2)$ chiral Lagrangian.

4.3. Chiral extrapolation assisted by the Omnès representation

We have achieved a representation of the form factor based on the Omnès representation, matched to low energy χ PT. Since we have relatively good theoretical control of the entire construction, we can now extrapolate to unphysical quark (pion) masses.

The parameterization in Eq. (5) requires two pieces of input: the pion scattering p -wave phase shift and the mean square radius. For the former we may either use the Breit–Wigner model – together with additional assumptions on the ρ properties – or the IAM, where the quark mass dependence is predicted from NLO χ PT – higher order pion mass dependencies as they arise from NNLO χ PT are not yet included.

The square radius has a NLO pion mass dependence caused by the chiral logarithm in \bar{l}_6 . This is a major effect for pion masses smaller than physical, towards the chiral limit, but for pion masses higher than physical (say the 330 MeV where the lattice data is taken), the m_π^2 term from the NNLO Lagrangian density might come to dominate, so we employ this too. Finally, we have an order-of-magnitude countercheck at our disposal. By employing a once-subtracted instead of a twice-subtracted Omnès representation, we obtain a closed form for the mean square radius in terms of the phase shift

$$\langle r^2 \rangle = \frac{6}{\pi} \int_{4m_\pi^2}^{\infty} ds \frac{\delta_{11}(s)}{s^2}. \quad (23)$$

All three methods are plotted in Fig. 4.

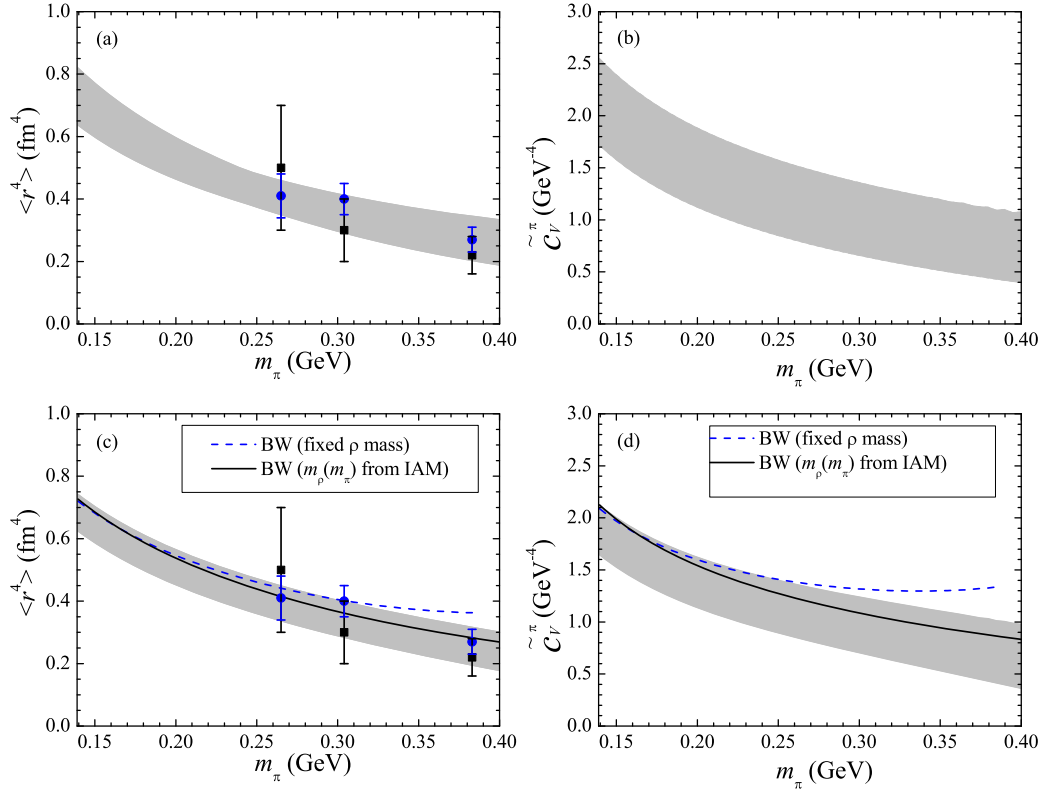


Fig. 5. Dependence on the pion mass of the mean quartic radius of the pion (left panel) and \tilde{c}_V^π (right panel). We show results based on the Breit–Wigner model (lower line) and the Inverse Amplitude Method (upper line). The bands correspond to the uncertainties from the parameters used (the \bar{l}_i 's for the IAM and the c_i (cf. Eq. (21)) for the Breit–Wigner) as well as from the variation of the cutoff. Also shown lattice data, that appeared after our results became public, are from [17]. The two data sets resulted from different methods to extract the curvature.

The results of the pion mass dependence of the quartic radius using the Breit–Wigner model and the IAM are plotted in Fig. 5(a) and (c), respectively, with the m_π dependence of the square radius coming from that of \bar{l}_6 as dictated by Eq. (16). In the IAM, the pion mass dependence of m_ρ is included intrinsically, while in the Breit–Wigner method, it is input from fitting to the recent lattice data [4] as described at the end of Section 4.1. The bands include the uncertainty from varying the parameters within one sigma and that from varying the integration cutoff from 1 to 16 GeV. The uncertainty from the cutoff is the dominant one. For comparison, we also plot the result of the Breit–Wigner model with fixed ρ mass as the dashed curve in Fig. 5(c). The dependence is smooth up to the point when the rho becomes stable. Here the curve ends. Imposing the m_π -dependent ρ mass as that given by the IAM, the result for the quartic radius in the Breit–Wigner model is shown as the solid curve in Fig. 5(c).

We can dispose altogether from the explicit pion mass dependence in $\langle r^2 \rangle$ by studying the quantity

$$\tilde{c}_V^\pi = c_V^\pi - \frac{1}{72} \langle r^2 \rangle^2.$$

This constant \tilde{c}_V^π can of course be also studied on a lattice by itself, although its physical interpretation is not transparent. But its mass dependence comes from the phase shift alone (cf. Eq. (6)), and is not compounded with the mass dependence of the square radius. It is therefore this quantity that allows most directly access to the pion mass dependence of the ρ properties. Our results for this quantity are shown in Fig. 5(b) and (d) using the IAM and the Breit–Wigner model, respectively.

5. Summary

Using the Omnès representation for the pion vector form factor, in this Letter we improved the existing value for the corresponding curvature using as input only the well-known $\pi\pi$ phase shifts in the p -wave as well as the pion radius. We find $\langle r^4 \rangle = 0.73 \pm 0.09 \text{ fm}^4$ or equivalently $c_V = 4.00 \pm 0.50 \text{ GeV}^{-4}$ which are consistent with the results from NNLO χ PT [14,18] and recent analysis using analyticity [21].

In addition we studied the pion mass dependence of the curvature. A modification of the curvature, called \tilde{c}_V^π in the Letter, can be represented solely by the $\pi\pi$ p -wave phase shift. We argued that this quantity allows for a clean and model-independent alternative access to the pion mass dependence of the ρ properties and would therefore provide a consistency check of the methods to extract physical parameters from lattice simulations. A lattice QCD study of the pion curvature would therefore be of high theoretical interest. We also argued that the pion square radius is not well suited for this kind of investigation, since additional, not so well controlled, theoretical input would be needed in the analysis. Quantities similar to \tilde{c}_V^π exist also for other form factors, and a study of them from both theoretical and lattice sides would be interesting.

Acknowledgements

We would like to thank Stephan Dürr and Jose Pelaez for useful discussions. This work is supported in part by grants FPA 2004-02602, 2005-02327, FPA2007-29115-E (Spain), and by the Helmholtz Association through funds provided to the virtual institute “Spin and strong QCD” (VH-VI-231). F.J.L.E. thanks the members of the IKP (Theorie) at Forschungszentrum Jülich for their

hospitality during the preparation of this work and the Fundacion Flores Valles for economical support.

References

- [1] M.E. Rose, Phys. Rev. 73 (1948) 279.
- [2] J. Gasser, U.-G. Meißner, Nucl. Phys. B 357 (1991) 90.
- [3] S. Aoki, et al., CP-PACS Collaboration, Phys. Rev. D 60 (1999) 114508; S. Dürr, et al., Science 322 (2008) 1224; C. Gattringer, et al., arXiv:0812.1681 [hep-lat]; P. Dimopoulos, et al., ETM Collaboration, arXiv:0810.1220 [hep-lat].
- [4] M. Gockeler, R. Horsley, Y. Nakamura, D. Pleiter, P.E.L. Rakow, G. Schierholz, J. Zanotti, arXiv:0810.5337 [hep-lat].
- [5] P.C. Bruns, U.-G. Meißner, Eur. Phys. J. C 40 (2005) 97, arXiv:hep-ph/0411223.
- [6] C. Hanhart, J.R. Pelaez, G. Rios, Phys. Rev. Lett. 100 (2008) 152001, arXiv:0801.2871 [hep-ph].
- [7] R.R. Akhmetshin, et al., JETP Lett. 84 (2006) 413, Pis'ma Zh. Eksp. Teor. Fiz. 84 (2006) 491, arXiv:hep-ex/0610016; R.R. Akhmetshin, et al., CMD-2 Collaboration, Phys. Lett. B 648 (2007) 28, arXiv:hep-ex/0610021.
- [8] A. Aloisio, et al., KLOE Collaboration, Phys. Lett. B 606 (2005) 12, arXiv:hep-ex/0407048.
- [9] M.N. Achasov, et al., J. Exp. Theor. Phys. 101 (2005) 1053, Zh. Eksp. Teor. Fiz. 101 (2005) 1201, arXiv:hep-ex/0506076.
- [10] E.P. Solodov, For the BaBar Collaboration, Study of e^+e^- collisions in the 1.5–3 GeV c.m. energy region using ISR at BaBar, in: D. Bettoni (Ed.), Proceedings of the 2001 e^+e^- Physics at Intermediate Energies Workshop, SLAC, Stanford, California, 30 April–2 May 2001, T03, arXiv:hep-ex/0107027.
- [11] S.R. Amendolia, et al., NA7 Collaboration, Nucl. Phys. B 277 (1986) 168.
- [12] J. Volmer, et al., Jefferson Lab F(pi) Collaboration, Phys. Rev. Lett. 86 (2001) 1713, arXiv:nucl-ex/0010009.
- [13] G.M. Huber, J. Phys. Conf. Ser. 69 (2007) 012015.
- [14] J. Bijnens, P. Talavera, JHEP 0203 (2002) 046, arXiv:hep-ph/0203049.
- [15] W.M. Yao, et al., Particle Data Group, J. Phys. G 33 (2006) 1.
- [16] P.A. Boyle, et al., JHEP 0807 (2008) 112, arXiv:0804.3971 [hep-lat].
- [17] After our paper was submitted to the preprint server, a new lattice analysis became public and we included the results in the revised version of the paper: R. Frezzotti, V. Lubicz, S. Simula, arXiv:0812.4042 [hep-lat].
- [18] J. Bijnens, G. Colangelo, P. Talavera, JHEP 9805 (1998) 014, arXiv:hep-ph/9805389.
- [19] P. Masjuan, S. Peris, J.J. Sanz-Cillero, Phys. Rev. D 78 (2008) 074028, arXiv:0807.4893 [hep-ph].
- [20] I. Caprini, Eur. Phys. J. C 13 (2000) 471, arXiv:hep-ph/9907227.
- [21] B. Ananthanarayan, S. Ramanan, arXiv:0811.0482 [hep-ph].
- [22] R. Omnès, Nuovo Cimento 8 (1958) 316.
- [23] M. Gimeno-Segovia, F.J. Llanes-Estrada, Eur. Phys. J. C 56 (2008) 557, arXiv:0805.4145 [hep-th].
- [24] H. Leutwyler, arXiv:hep-ph/0212324.
- [25] S.J. Brodsky, G.R. Farrar, Phys. Rev. D 11 (1975) 1309.
- [26] F.J. Llanes-Estrada, F.-K. Guo, C. Hanhart, U.-G. Meißner, PoS EFT09 (2009) 054.
- [27] F. Guerrero, Phys. Rev. D 57 (1998) 4136; F. Guerrero, A. Pich, Phys. Lett. B 412 (1997) 382.
- [28] J.A. Oller, L. Roca, Phys. Lett. B 651 (2007) 139, arXiv:0704.0039 [hep-ph].
- [29] J.A. Oller, E. Oset, J.E. Palomar, Phys. Rev. D 63 (2001) 114009, arXiv:hep-ph/0011096.
- [30] J. Gasser, H. Leutwyler, Ann. Phys. 158 (1984) 142; S. Weinberg, Physica A 96 (1979) 327.
- [31] A. Dobado, M.J. Herrero, T.N. Truong, Phys. Lett. B 235 (1990) 134.
- [32] T.N. Truong, Phys. Rev. Lett. 61 (1988) 2526.
- [33] F. Guerrero, J.A. Oller, Nucl. Phys. B 537 (1999) 459, arXiv:hep-ph/9805334; F. Guerrero, J.A. Oller, Nucl. Phys. B 602 (2001) 641, Erratum.
- [34] G. Ecker, J. Gasser, A. Pich, E. de Rafael, Nucl. Phys. B 321 (1989) 311; F.J. Llanes-Estrada, P. De A. Bicudo, Phys. Rev. D 68 (2003) 094014, arXiv:hep-ph/0306146; T.N. Pham, T.N. Truong, Phys. Rev. D 31 (1985) 3027; F.J. Yndurain, arXiv:hep-ph/0212282; M.R. Pennington, J. Portoles, Phys. Lett. B 344 (1995) 399.
- [35] A. Dobado, J.R. Pelaez, Phys. Rev. D 56 (1997) 3057, arXiv:hep-ph/9604416.
- [36] G. Colangelo, J. Gasser, H. Leutwyler, Nucl. Phys. B 603 (2001) 125, arXiv:hep-ph/0103088.
- [37] A. Dobado, et al., Effective Lagrangians for the Standard Model, Springer-Verlag, Berlin, Heidelberg, 1997.
- [38] T.B. Bunton, F.J. Jiang, B.C. Tiburzi, Phys. Rev. D 74 (2006) 034514, Phys. Rev. D 74 (2006) 099902, Erratum.